Electronic Supplementary Material (ESI) for ChemComm.

Supporting Information for:

Direct electrochemical identification of rare microscopic catalytic active sites

Cameron L. Bentley,[*a] *Lachlan F. Gaudin*[a] *and Minkyung Kang*[b]

[a]School of Chemistry, Monash University, Clayton, Victoria 3800, Australia

[b]Institute for Frontier Materials Deakin University, Burwood, Victoria 3125, Australia

*E-mail: cameron.bentley@monash.edu

Contents

Section S1. Experimental section

Chemical reagents and electrode materials. Perchloric acid ($HClO_4$, 70%, Sigma-Aldrich) and potassium chloride (KCl, 99.5%, Sigma-Aldrich) were used as supplied by the manufacturer. All aqueous solutions were prepared with ultrapure deionised water (resistivity = 18.2 MΩ·cm at 25 °C, Direct-Q Water Purification System, Milli-Q, USA).

The natural crystal of molybdenite (2H-MoS_2) was purchased from SPI Supplies (USA) and was prepared as previously reported.[1] Prior to use as an electrode material, the bulk crystal of MoS_2 was fixed on a glass substrate using a double-sided tape and then mechanically cleaved through the "scotch-tape method".[2] To ensure electrical connection, the freshly cleaved MoS_2 flakes were top contacted with adhesive copper tape. Note that all experiments were completed right after cleavage to avoid deterioration from exposure to the ambient atmosphere.

Ag/AgCl quasi-reference counter electrodes (QRCEs) were prepared by anodizing 125 μm diameter Ag wire (99.99%, Goodfellow, U.K.) in an aqueous saturated KCl solution. The Ag/AgCl QRCEs possessed a stable reference potential of +0.222 ± 0.005 V vs. commercial saturated calomel electrode (SCE) on the hours timescale in 0.1 M $HClO_4$, consistent with a previous report.[3] Note that unless otherwise stated, all potentials are calibrated (corrected) to the SCE scale, herein.

Probe fabrication and size calibration. The single channelled nanopipette probes were fabricated from filamented borosilicate glass capillaries (BF100-50-10, Sutter Instruments, USA) using a Narishige PC-100 vertical puller (Narishige Group, Japan). After fabrication, the probes were back-filled with analyte solution (*e.g.*, 0.1 M $HClO_4$) using a MicroFil syringe (World Precision Instruments Inc., USA), before adding a thin layer of silicone oil (Sigma-Aldrich) on top to minimize evaporation from the back of the nanopipette during prolonged scanning, as previously reported.[4] Ag/AgCl QRCEs were then inserted through the silicone oil layer into the analyte solution to finalize the SECCM probe, rendering it ready for use.

A one stage, 4 weight (2 light and 2 heavy, 250 g total) program was designed, and the puller power was varied between 55 and 69 (A.U.) to create triplicate probes at each power. These probes were filled with a 0.1 M KCl solution, equipped with an Ag/AgCl QRCE, and then the tip of this probe was placed in an electrolyte bath (also containing 0.1 M KCl), emulating the experimental set up used in scanning ion conductance microscopy (SICM).[5] The tip resistance (R_{tip}) of these probes was estimated by performing a voltage sweep between ±0.1 V, as previously reported,[6] and a calibration curve was constructed, as shown in Figure S1.

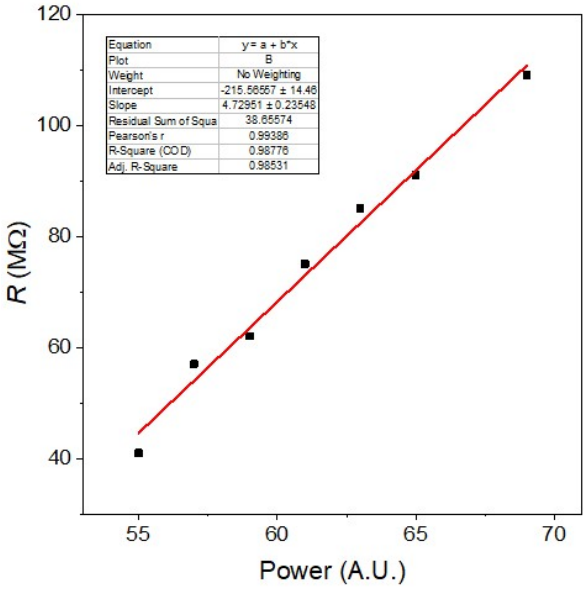

Figure S1. Calibration curve of the probe resistance (*R*) measured in 0.1 M KCl (aq) versus the power used to pull the probe.

Evidently, there is a strong linear relationship (R^2 = 0.99) between the measured resistance (dominated by R_{tip}) and the puller power. R_{tip} is inversely related to the tip radius, r_{tip} through the following relationship:[6]

$$R_{tip} \approx \frac{\rho}{\pi r_t \tan \beta} + \frac{\rho}{4 r_{tip}} \qquad \textbf{(S1)}$$

where β is the inner cone angle and ρ is the solution resistivity. Thus, if it is assumed that β is relatively constant across the investigated power range, r_{tip} is approximately inversely proportional to the puller power. To confirm whether this is a valid approximation, selected probes across the power range were

subjected to imaging with scanning electron microscopy (SEM) to directly estimate r_{tip}. A calibration plot of R_{tip} vs. $1/r_{tip}$ is shown in Figure S2. The strong linear relationship (R^2 = 0.96) confirms the assumption made above, meaning r_{tip} can be calculated approximately from the puller power (Figure S1) or more accurately from measuring R (Figure S2). The probes used herein were pulled at a power of 61 A.U. and had a resistance of ≈70 – 75 MΩ, corresponding to a tip radius and area of *ca.* 0.067 μm and 0.014 μm^2, respectively.

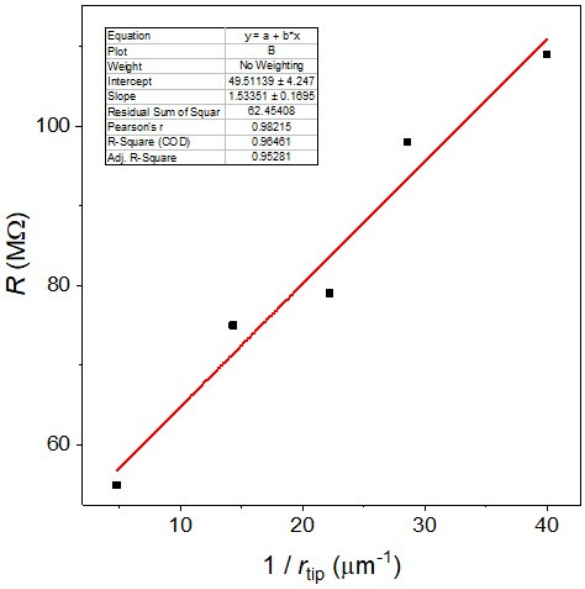

Figure S2. Calibration curve of the probe resistance (R) measured in 0.1 M KCl (aq) versus the inverse of tip radius ($1/r_{tip}$), measured using SEM.

Environmental control. Environmental (atmospheric) control was achieved using a previously reported environmental cell design,[7] with slight modifications. A polypropylene container (HPL931, 100 mL, Lock&Lock, South Korea; dimensions 9 × 8.6 × 7.8 cm^3), modified with a gas inlet port (Omnifit Connector, Kinesis, UK) enabled the supply of N_2 to "degas" the SECCM droplet cell during measurement. The N_2 was passed through a bubbler containing saturated NaCl to fix the relative humidity of the incoming gas stream at ~75%, before passing through a variable area flow meter (2510 2A12, Brooks Instrument, USA) to maintain a constant flux (flow rate ≈ 100 sccm) into the environmental cell. Three separate holes were made in the lid of the cell, a circular hole of ~4 mm diameter in the middle of the lid to enable the approach of the SECCM probe while maintaining a

positive gas overpressure inside of the environmental cell (note that further sealing around the probe was found to be not necessary, as discussed below). Two other circular holes on either side of ~2 cm in diameter were replaced with cover glass to allow for both light to access as well as providing an optical pathway to enable viewing of the probe tip and working electrode (WE) surface with an optical camera (*vide infra*).

To confirm that the SECCM droplet cell had been completely purged of O_2, local cyclic voltammetric measurements were made on the surface of a polished polycrystalline platinum foil electrode, as shown in Figure S3. Evidently, while the oxygen reduction reaction (ORR) wave is quite prominent under ambient air (red trace, in agreement with previous reports[8, 9]), there is no trace of this process under the N_2 atmosphere (blue trace), confirming the efficacy of the environmental cell.

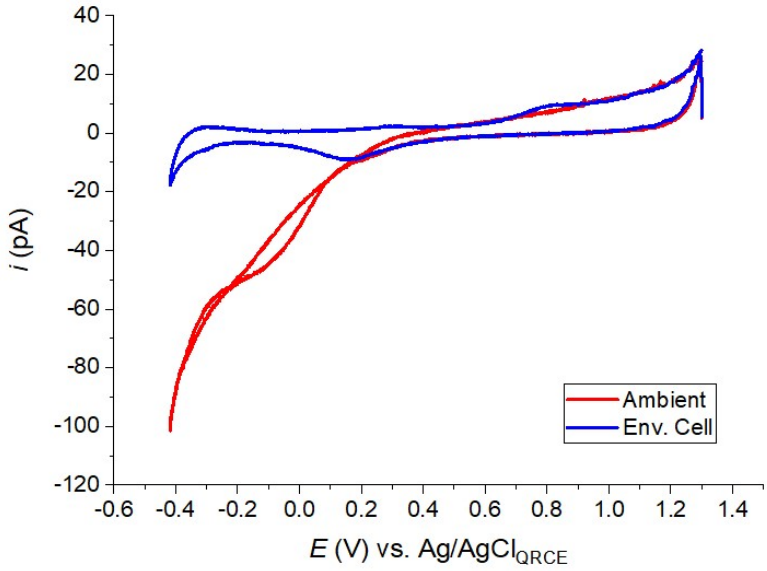

Figure S3. Cyclic voltammograms (voltammetric scan rate, υ = 0.5 V s^{-1}) obtained at a polycrystalline Pt surface under ambient (red curve) and N_2-purged (blue curve) conditions. These experiments were carried out in the SECCM format, with a nanopipette probe that had a tip area of ~0.014 μm^2 and contained 0.1 M $HClO_4$.

Scanning electrochemical cell microscopy (SECCM). Local electrochemical measurements were carried out in the SECCM format on a home-built scanning electrochemical probe microscopy (SEPM) workstation, as previously reported.[10-13] In this configuration, the constructed SECCM probe (*i.e.*, filled

nanopipette equipped with QRCE, *vide supra*) was mounted on an *xyz*-piezoelectric positioner (200 × 200 × 200 µm range, Nano-3D200, MadCityLabs, USA) and the MoS_2 WE was loaded into the environmental cell. After placing the lid on the environmental cell, it was purged under a continuous flow of N_2 and the SECCM probe was initially positioned above the WE using coarse *xyz*-micropositioners (9064-XYZ-M, Newport, USA) in tandem with an optical camera (Axiocam ERc 5s, ZEISS, Germany) fitted with a magnification lens (44mm/3.0× InfiniStix, Infinity USA).

The SECCM probe was approached to MoS_2 surface using a surface current (i_{surf}) threshold of *ca.* 2.5 pA to detect when the droplet-surface contact had been made and to stop further translation. Note that the probe itself never contacted the MoS_2 surface. Electrochemical measurements (linear sweep voltammetry, herein) were performed in the confined area defined by the droplet cell created between the SECCM probe tip and MoS_2 surface. Mapping was carried out using a standard voltammetric *hopping mode protocol*, as previously reported.[14, 15] In brief, the SECCM probe was approached to the MoS_2 surface at a series of locations in a predefined grid pattern and, upon each landing, an independent linear sweep voltammetry measurement was made, building up spatially-resolved electrochemical (*current–potential*) 'images' of the substrate surface. In addition, the final position of the *z*-piezoelectric positioner at approach was used to synchronously construct a topographical map of MoS_2 surface.

The SEPM set up was located on a vibration isolation platform (25BM-8, Minus K, USA) localised within an aluminium faraday cage equipped with acoustic foam, to minimize mechanical vibration and electrical noise during prolonged scanning.[16, 17] The QRCE potential was controlled, with respect to ground and the current flowing at the MoS_2 WE surface (*i.e.*, i_{surf}), held at a common ground, was measured with a variable-gain low-noise current amplifier (DLPCA-200, FEMTO, Germany). i_{surf} was measured every 4 µs, and averaged in 512 blocks to give an effective data acquisition rate of 4 × (512 + 1) = 2052 µs, where one extra iteration was used to transfer the data to the host computer. An in-line low-pass electrical filter (1 kHz, EF110, Thorlabs, USA) was utilized during data (current) collection.

Instrumental control and data acquisition was carried out using an FPGA card (NI USB-7855R) controlled by a LabVIEW 2020 (National Instruments, USA) interface running the Warwick Electrochemical Scanning Probe Microscopy (WEC-SPM, www.warwick.ac.uk/electrochemistry) software.

Data analysis and processing. After acquisition, the raw SECCM data were processed using the Matlab R2020a (Mathworks, USA) software package. Data plotting was carried out using the Matlab R2020 and OriginPro 2019b (OriginLab, USA) software packages. Note that all electrochemical maps and movies are presented without any data interpolation.

Maps of the maximum catalytic current (i_{max}) were constructed by extracting the current obtained at the "final potential" of the spatially-resolved LSVs (*e.g.*, at −1.13 V vs. SCE in Figure 1 of the main text). During this procedure, outliers were discarded by first applying a moving median filter (window = 5 points) to the data.

Fitting of the spatially-resolved *i–E* data was carried out with the following exponential function:

$$y = y_0 + A \cdot exp(R_0 \cdot x) \quad \text{(S1)}$$

This model is analogous to the Butler-Volmer equation for an electrochemically irreversible process, where the pre-exponential factor, A, scales with the heterogeneous electron-transfer rate constant (k^0) and the constant, y_0, accounts for nonfaradaic contributions (e.g., double layer charging) to the overall current.[18] Using this approach, a fitted plot of the potential required to achieve 10 mA cm^{-2} (*E* @ 10 mA cm^{-2}) was constructed, as shown below in Section S2.

Data binning and trinarisation. As described in the main text, data trinarisation was performed by binning the i_{max} with respect to the median i_{max} value (note that the median was used rather than the mean to avoid skewing of the result by the highly active SE pixels). The three bins were assigned heuristically based on the distributions (histograms) of i_{max}, shown in Figure 1d in the main text and

reproduced below for convenience (Figure S4). The upper and lower bins of $|i_{max}| \leq |1.5 \cdot i_{max,median}|$ and $|i_{max}| > |15 \cdot i_{max,median}|$, shown in Figure S4, conveniently divide the data into BP and SE, respectively, with the intermediate bin of $|1.5 \cdot i_{max,median}| < |i_{max}| \leq |15 \cdot i_{max,median}|$ containing "everything else", allowing the active regions of BP3 and active pixels of BP2 to be readily identified. Note that in Figure S4, calculating the $i_{max,median}$ value of −2.88 pA ($\log_{10}|i_{max,median}| = -11.54$) gives $1.5 \cdot i_{max,median}$ and $15 \cdot i_{max,median}$ bin limits of −4.32 pA (−11.36) and −43.2 pA (−10.36), respectively.

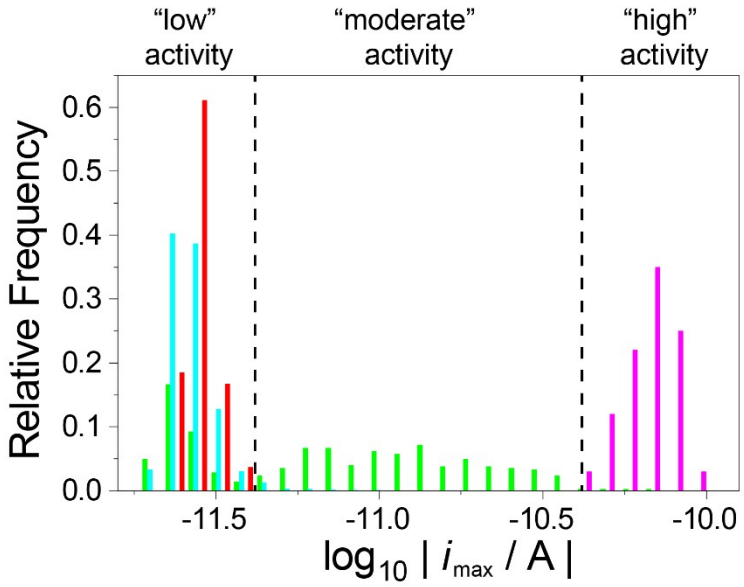

Figure S4. Normalised histograms of i_{max}, extracted from the corresponding regions marked in the main text, Figure 1b (BP1, BP2, BP3 and SE correspond to red, cyan, green and magenta, respectively). Normalised histograms were constructed by dividing number of counts (N) by the total number of counts (N_{total}) for a given distribution. N_{total} is 54, 2128, 422 and 100 for BP1, BP2, BP3 and SE, respectively. The "low", "moderate" and "high" activity bins represent: $\log_{10}|i_{max}| \leq -11.36$, $-11.36 < \log_{10}|i_{max}| \leq -10.36$ and $\log_{10}|i_{max}| > -10.36$, respectively.

Surface characterisation and imaging. Optical imaging was completed on a reflection mode optical microscopy system (Axiolab 5, ZEISS, Germany) fitted with an Axiocam 105 color camera and processed using ZEN imaging software. Post-scan co-located imaging of the SECCM scan area was completed on an FEI Quanta FEGSEM (FEI, USA), operated with an Everhart–Thornley detector (ETD) in the secondary electron and backscattered electron modes. Measurement of probe tip radii was completed via coating the probes with gold at a thickness of ~5 nm.

Section S2. Extended analysis of SECCM data

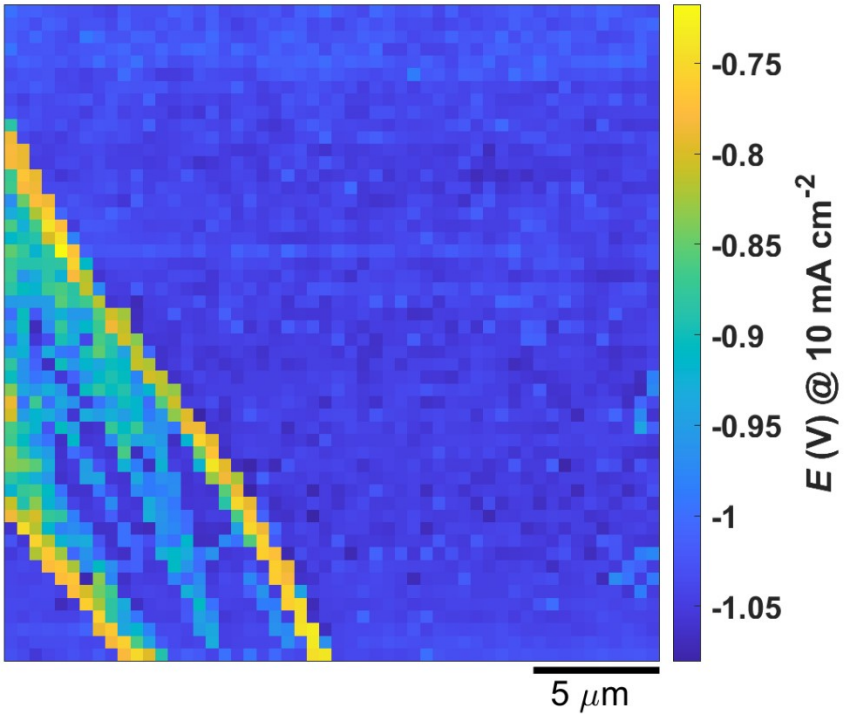

Figure S5. Spatially-resolved map of potential required to achieve a current density of 10 mA cm^{-2} (*E* @ 10 mA cm^{-2}). This map was constructed by exponential fitting of the spatially-resolved *i*–*E* data (details provided in Section S1) extracted from Movie S1. The SECCM probe contained 0.1 M $HClO_4$. Tip radius, tip area and hopping distance were ~0.067 µm, ~0.014 $µm^2$ and 0.5 µm, respectively.

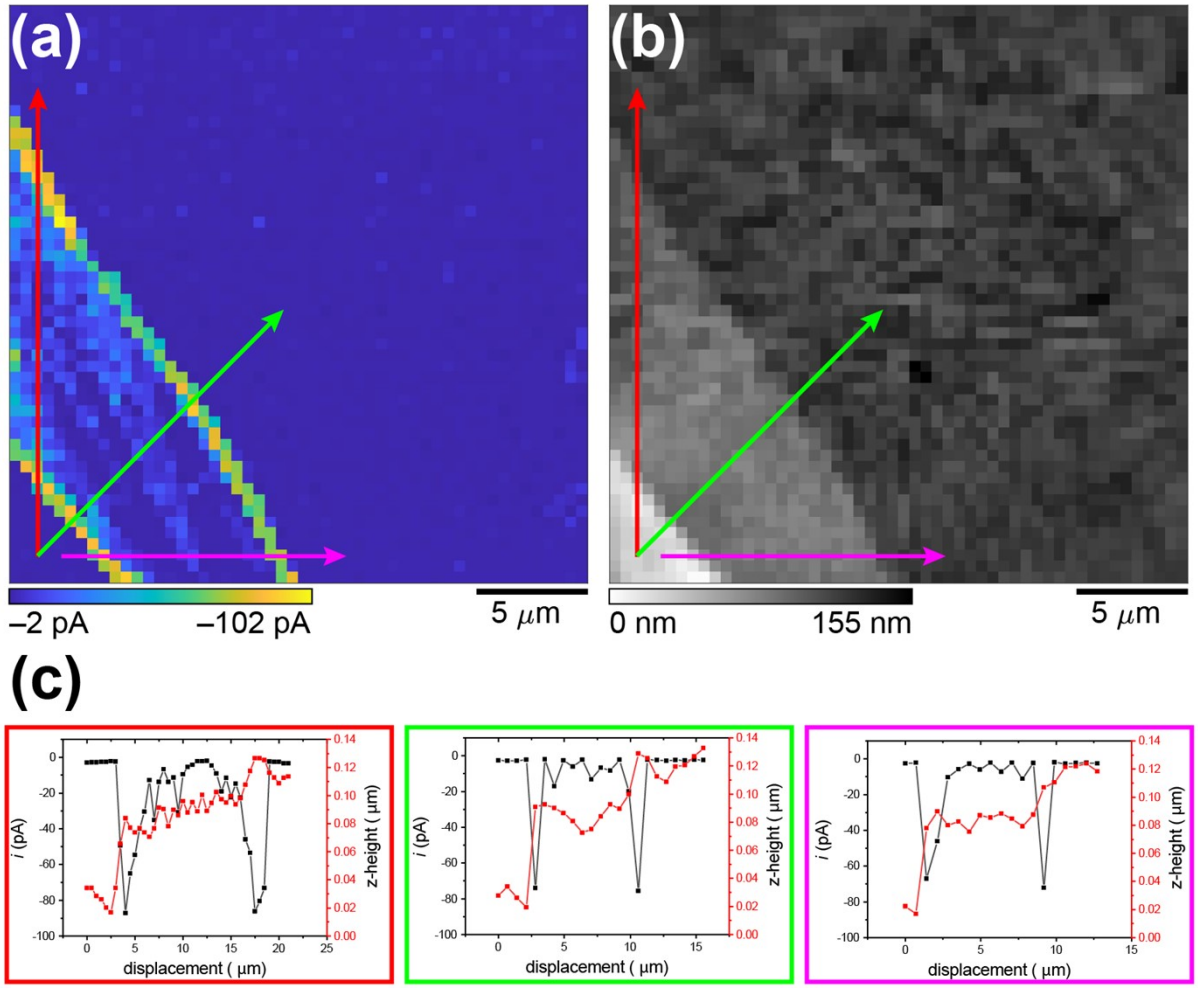

Figure S6. Spatially-resolved maps of **(a)** i_{max} (full *i*–*E* data available in Movie S1) and **(b)** topography, obtained from the surface of 2H-MoS_2. **(c)** Line scans of i_{surf} (left axis, black) and topography (right axis, red) obtained along the lines indicated in (a) and (b). The SECCM probe had a tip area of ~0.014 μm^2 and contained 0.1 M $HClO_4$.

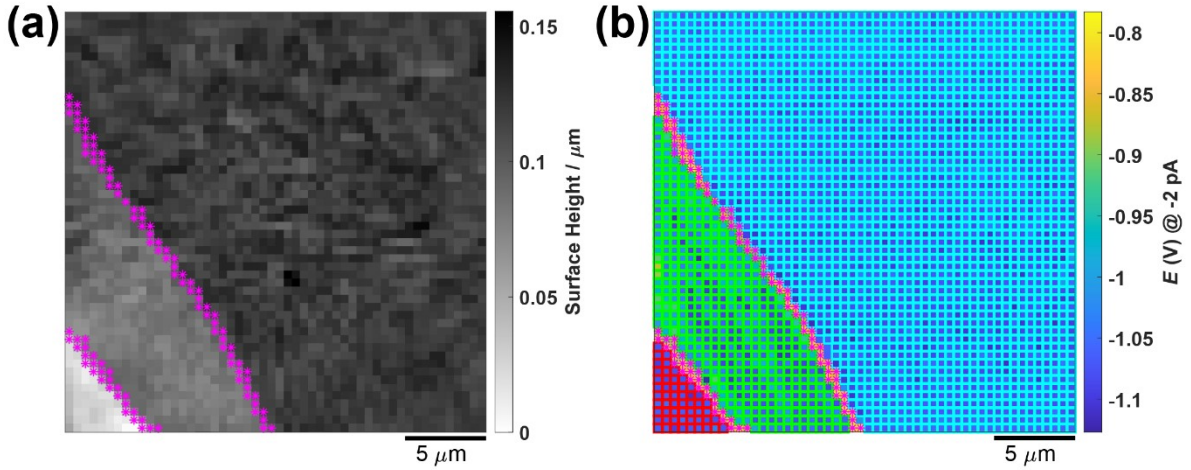

Figure S7. Spatially-resolved maps of **(a)** topography and **(b)** electrochemical activity, obtained from the surface of 2H-MoS_2. Pixel selections used to construct Figure 1c and d in the main text are indicated, with red, cyan, green and magenta pixels corresponding to BP1, BP2, BP3 and SE, respectively.

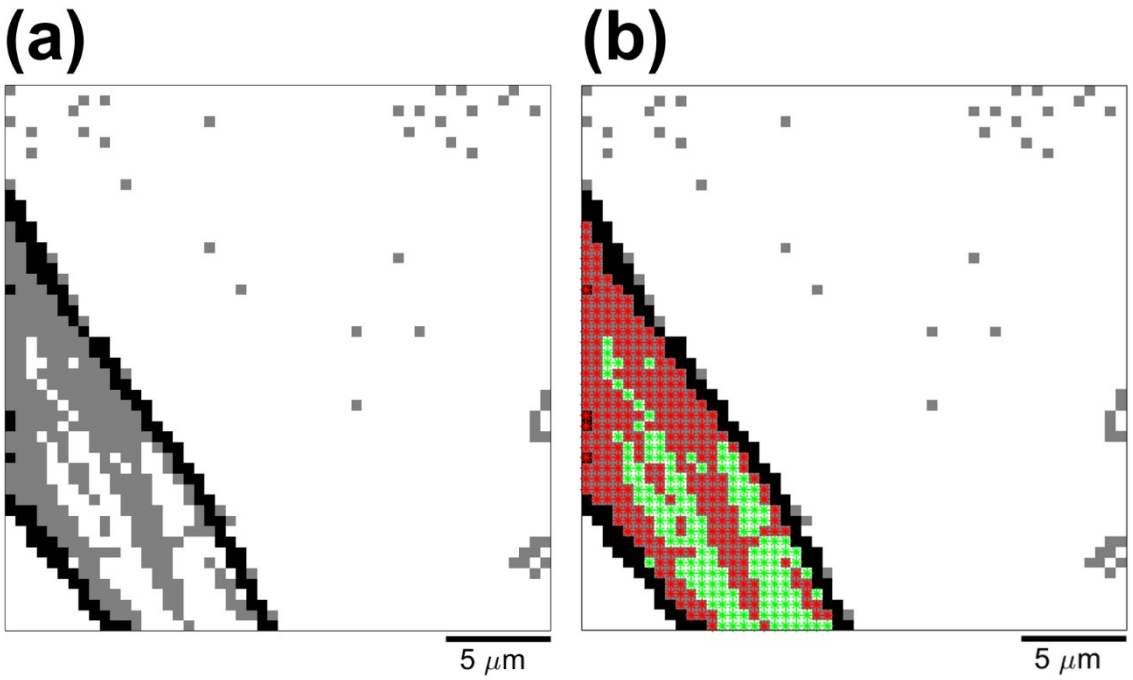

Figure S8. (a) Unlabelled and **(b)** labelled trinarised images of $|i_{max}|$, obtained from the surface of 2H-MoS_2. Pixel selections used to construct Figure 2e in the main text are indicated in (b), with green and red corresponding to "low" and "moderate" activity, respectively.

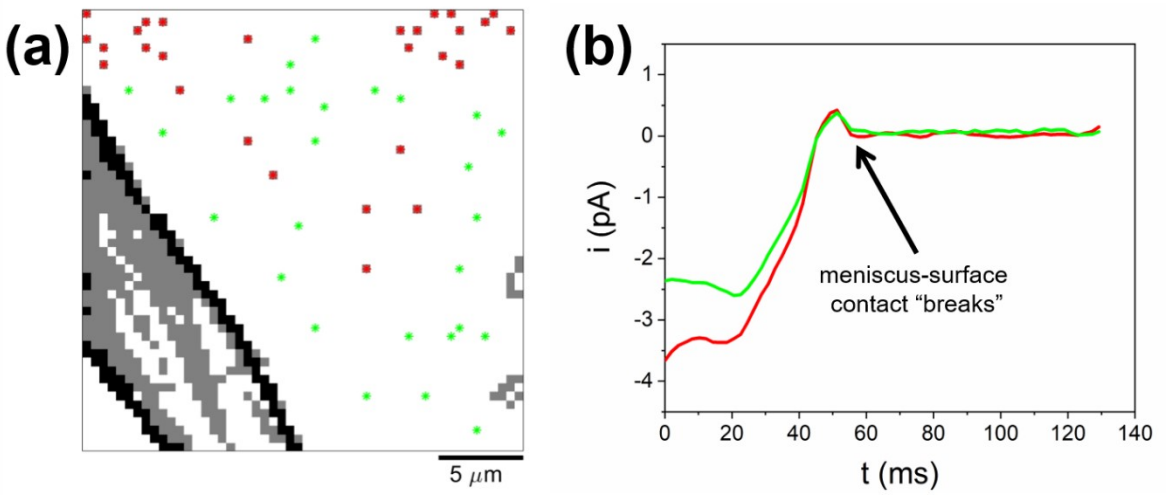

Figure S9. (a) Trinarised image of $|i_{max}|$, where white, grey and black pixels represent: $|i_{max}| \leq |1.5 \cdot i_{max,median}|$, $|1.5 \cdot i_{max,median}| < |i_{max}| \leq |15 \cdot i_{max,median}|$ and $|i_{max}| > |15 \cdot i_{max,median}|$, respectively. **(b)** Mean retract transients (*i.e.*, current-time during retract) obtained from the electrocatalytic "hot spots" [N = 27, labelled red in (a)] and random points across BP2 [N = 27, labelled green in (b)]. The potential during retract was −1.13 V vs. SCE.

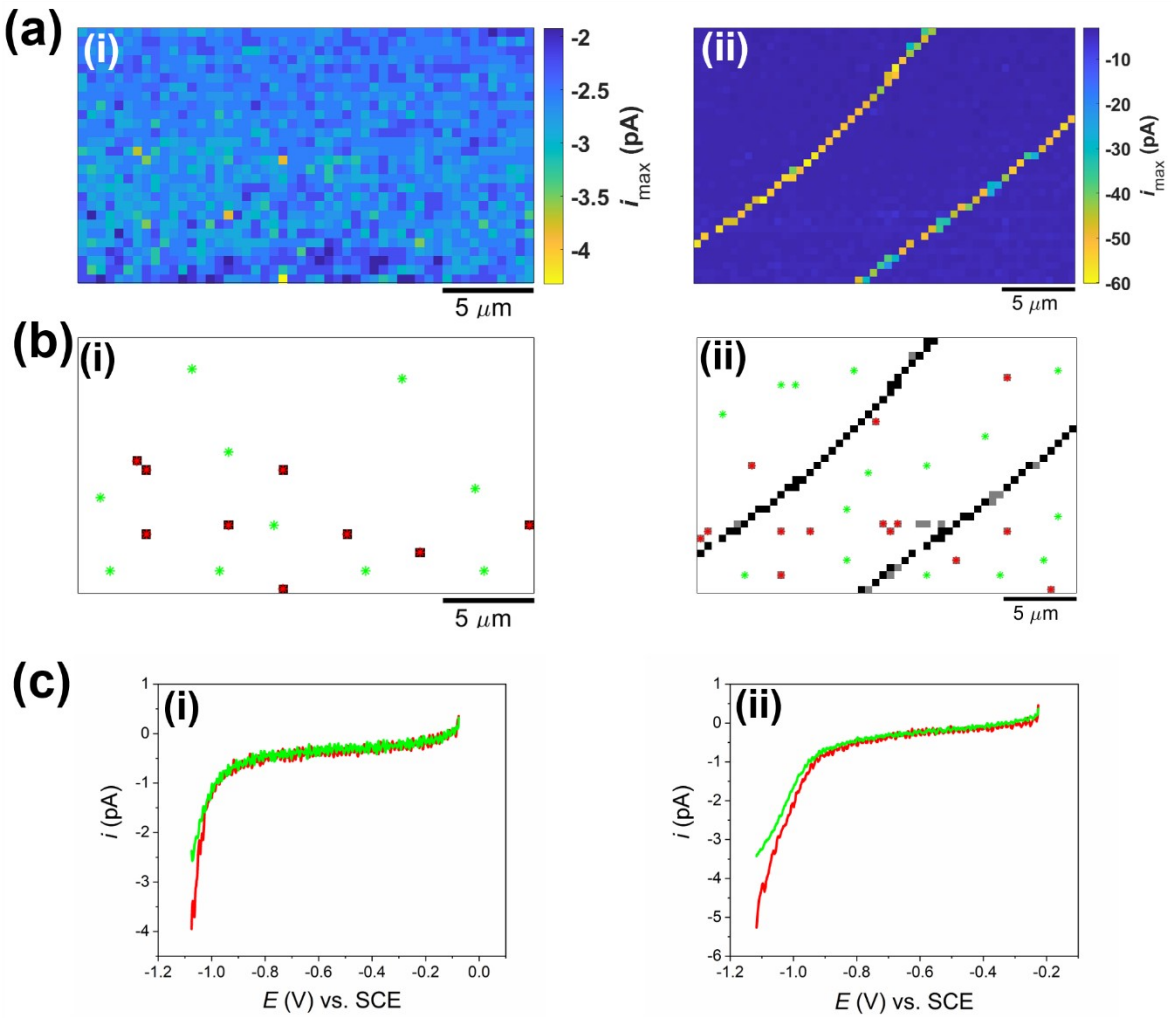

Figure S10. (a) Spatially-resolved map of i_{max}, **(b)** trinarised image of $|i_{max}|$ and **(c)** mean LSVs (υ = 1 V s^{-1}) extracted from the corresponding green and red pixels, labelled in (b), obtained from the surface of 2H-MoS_2. **(i)** 1400 pixels over a 25 × 14 μm^2 scan area (hopping distance = 0.5 μm). **(ii)** 1750 pixels over a 26 × 17.5 μm^2 scan area (hopping distance = 0.5 μm). (i) and (ii) correspond to two different electrodes/crystals. The LSVs shown in (c) were extracted from electrocatalytic "hot spots" [(i) N = 9 and (ii) N = 14, labelled red in (b)] and random points across the BP [(i) N = 10 and (ii) N = 15, labelled green in (c)]. The "hot spots" are present at pixel and areal densities of *ca.* (i) 0.6% and 0.5 μm^{-2}, respectively and (ii) 0.8% and 0.6 μm^{-2}, respectively.

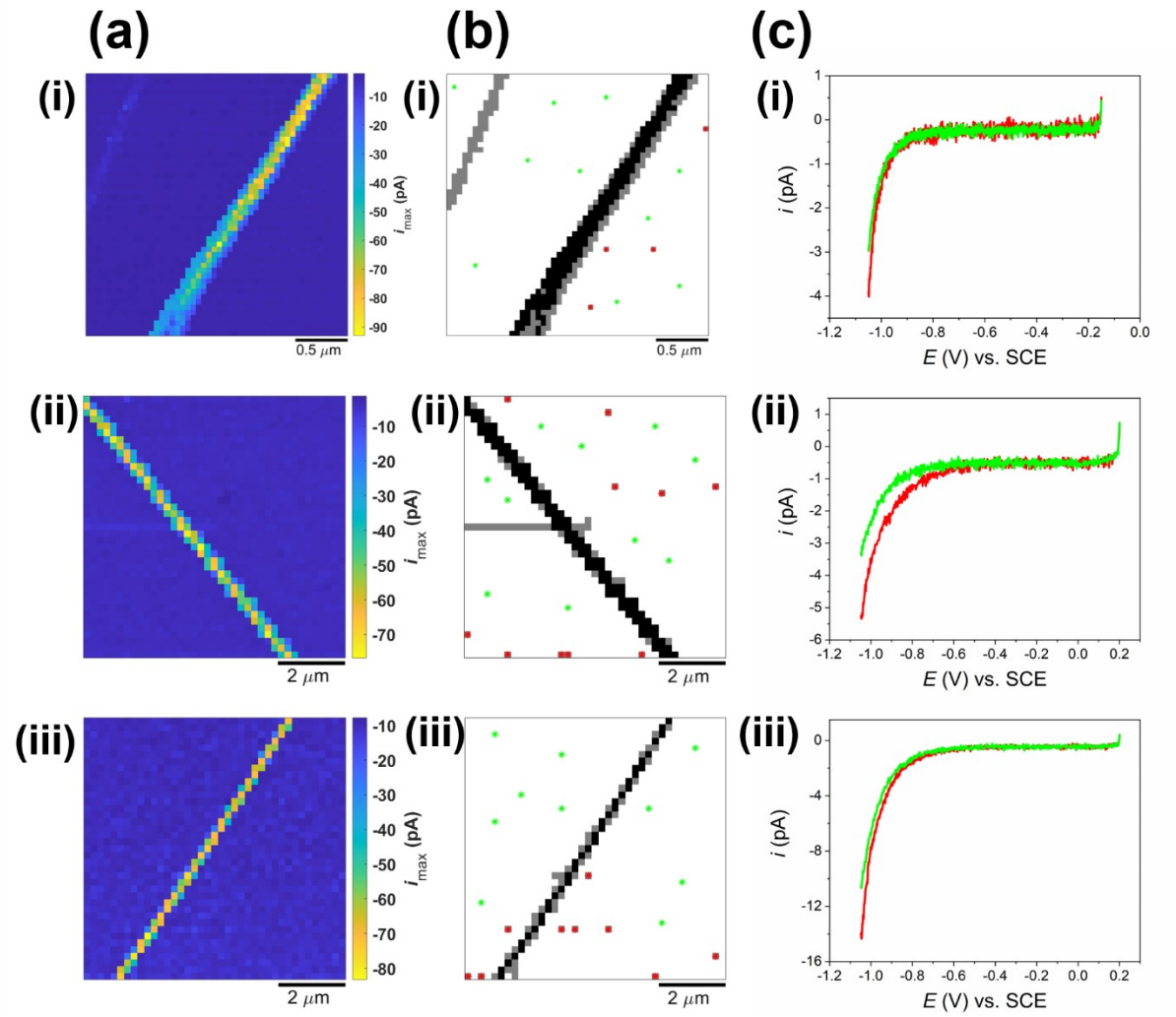

Figure S11. (a) Spatially-resolved map of i_{max}, **(b)** trinarised image of $|i_{max}|$ and **(c)** mean LSVs (υ = 1 V s^{-1}) extracted from the corresponding green and red pixels, labelled in (b), obtained from the surface of 2H-MoS_2. **(i)** 2500 pixels over a 2.5 × 2.5 μm^2 scan area (tip radius = 0.015 μm, hopping distance = 0.05 μm), adapted with permission from the study by Bentley et al.[16] Copyright 2017 American Chemical Society. **(ii)** and **(iii)** 1600 pixels over a 20 × 20 μm^2 scan area (tip radius = 0.07 μm, hopping distance = 0.2 μm), adapted with permission from the study by Tao et al.[1] Copyright 2020 American Chemical Society. (i), (ii) and (iii) correspond to three different electrodes/crystals. The LSVs shown in (c) were extracted from electrocatalytic "hot spots" [(i) N = 4, (ii) N = 10 and (iii) N = 9, labelled red in (b)] and random points across the BP [N = 10, labelled green in (c)]. In all cases, the SECCM probe contained 0.1 M $HClO_4$.

Section S3. Additional SEM Images of the SECCM scan areas

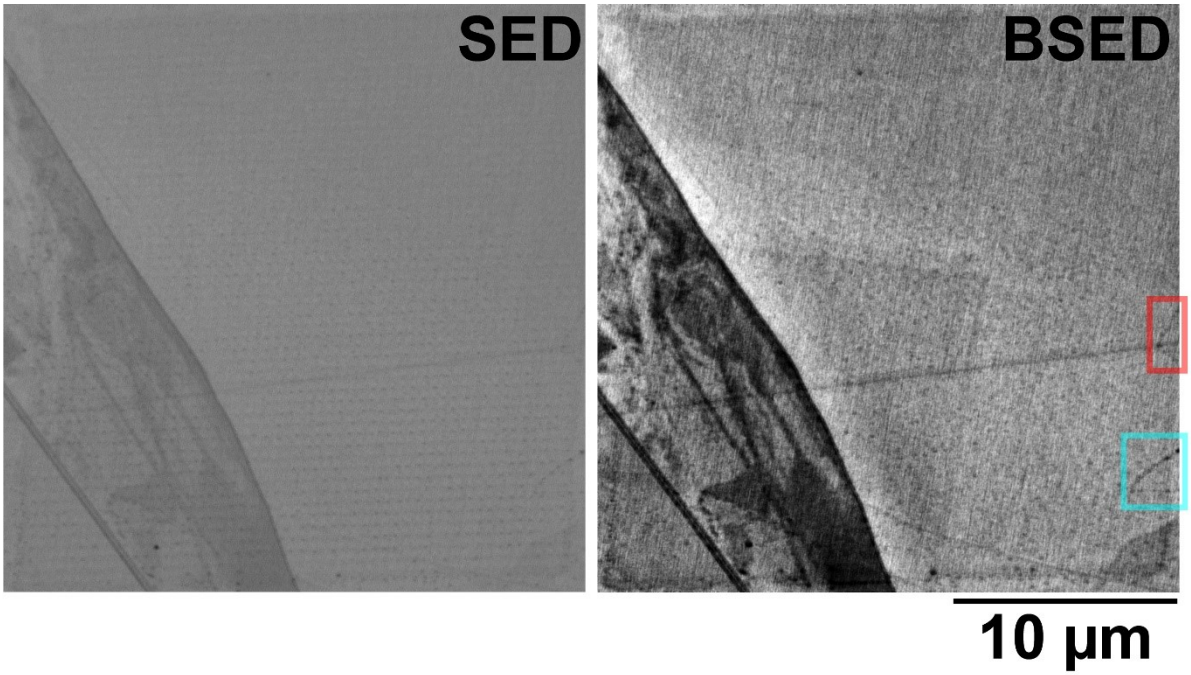

Figure S12. Co-located SEM image of an entire SECCM scan area (see main text, Figure 1), shown with secondary electron (left, SED) and backscattered electron (right, BSED) detectors. The two active structures identified with SECCM (main text, Figure 3) are delineated by red and cyan boxes.

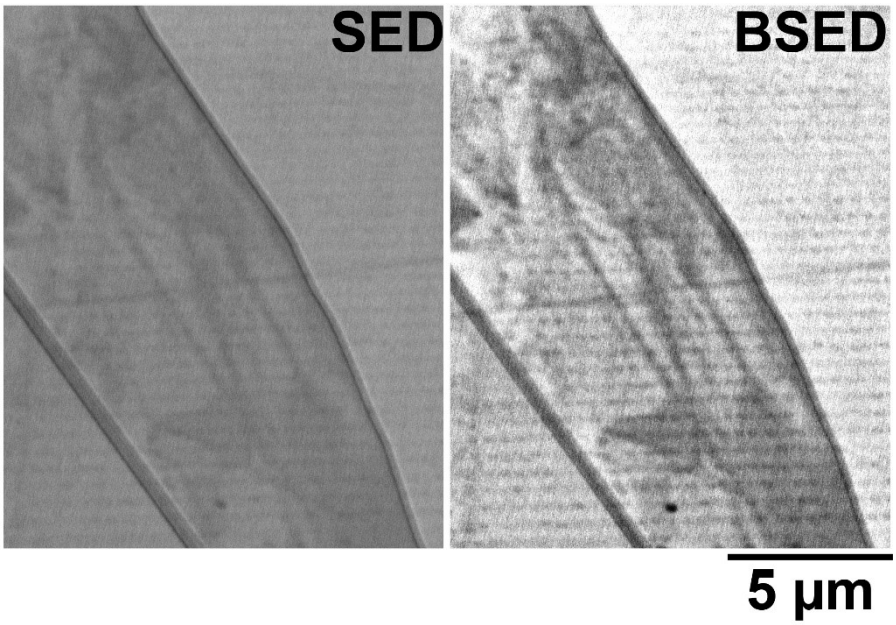

Figure S13. Co-located SEM image of a zoomed-in region of an SECCM scan area (i.e., BP3, see main text, Figure 2), shown with secondary electron (left, SED) and backscattered electron (right, BSED) detectors.

Section S4. Movie captions

Movie S1. Spatially-resolved electrochemical movie (2704 pixels over a 26 × 26 μm^2 scan area) obtained with the voltammetric hopping mode SECCM protocol, visualizing HER activity on an exfoliated surface of molybdenite (2H-MoS_2). The SECCM probe had a tip area of ~0.014 μm^2 and contained 0.1 M $HClO_4$. Experimental parameters were as follows: voltammetric scan rate (υ) = 1 V s^{-1}, approach voltage (E_a) = –1.35 V, initial potential (E_i) = –0.45 V and final potential (E_f) = –1.35 V (all vs. Ag/AgCl QRCE). The data presented are not interpolated. The data contained in this movie were used to construct Figures 1 – 3 in the main text.

Movie S2. Spatially-resolved electrochemical movie (2704 pixels over a 26 × 26 μm^2 scan area) obtained with the voltammetric hopping mode SECCM protocol, visualizing HER activity on an exfoliated surface of molybdenite (2H-MoS_2). The SECCM probe had a tip area of ~0.014 μm^2 and contained 0.1 M $HClO_4$. Experimental parameters were as follows: υ = 1 V s^{-1}, E_a = –1.35 V, E_i = –0.45 V and E_f = –1.35 V (all vs. Ag/AgCl QRCE). The data presented are not interpolated. The data contained in this movie were used to construct Figure 4 in the main text.

SI References

1. Tao, B.; Unwin, P. R.; Bentley, C. L., Nanoscale Variations in the Electrocatalytic Activity of Layered Transition-Metal Dichalcogenides. *The Journal of Physical Chemistry C* **2020,** *124* (1), 789-798.
2. Novoselov, K. S.; Geim, A. K.; Morozov, S. V.; Jiang, D.; Zhang, Y.; Dubonos, S. V.; Grigorieva, I. V.; Firsov, A. A., Electric Field Effect in Atomically Thin Carbon Films. *Science* **2004,** *306* (5696), 666-669.
3. Bentley, C. L.; Perry, D.; Unwin, P. R., Stability and Placement of Ag/AgCl Quasi-Reference Counter Electrodes in Confined Electrochemical Cells. *Analytical Chemistry* **2018,** *90* (12), 7700-7707.
4. Bentley, C. L.; Kang, M.; Maddar, F. M.; Li, F.; Walker, M.; Zhang, J.; Unwin, P. R., Electrochemical Maps and Movies of the Hydrogen Evolution Reaction on Natural Crystals of Molybdenite (MoS_2): Basal vs. Edge Plane Activity. *Chem. Sci.* **2017,** *8* (9), 6583-6593.
5. Zhu, C.; Huang, K.; Siepser, N. P.; Baker, L. A., Scanning Ion Conductance Microscopy. *Chem Rev* **2020**.
6. Perry, D.; Momotenko, D.; Lazenby, R. A.; Kang, M.; Unwin, P. R., Characterization of Nanopipettes. *Analytical Chemistry* **2016,** *88* (10), 5523-5530.
7. Ornelas, I. M.; Unwin, P. R.; Bentley, C. L., High-Throughput Correlative Electrochemistry−Microscopy at a Transmission Electron Microscopy (TEM) Grid Electrode. *Analytical Chemistry* **2019,** *91* (23), 14854-14859.
8. Chen, C.-H.; Meadows, K. E.; Cuharuc, A.; Lai, S. C. S.; Unwin, P. R., High Resolution Mapping of Oxygen Reduction Reaction Kinetics at Polycrystalline Platinum Electrodes. *Phys. Chem. Chem. Phys.* **2014,** *16* (34), 18545-18552.
9. Ustarroz, J.; Ornelas, I. M.; Zhang, G.; Perry, D.; Kang, M.; Bentley, C. L.; Walker, M.; Unwin, P. R., Mobility and Poisoning of Mass-Selected Platinum Nanoclusters during the Oxygen Reduction Reaction. *ACS Catalysis* **2018,** *8* (8), 6775-6790.
10. Snowden, M. E.; Güell, A. G.; Lai, S. C. S.; McKelvey, K.; Ebejer, N.; O'Connell, M. A.; Colburn, A. W.; Unwin, P. R., Scanning Electrochemical Cell Microscopy: Theory and Experiment for Quantitative High Resolution Spatially-Resolved Voltammetry and Simultaneous Ion-Conductance Measurements. *Analytical Chemistry* **2012,** *84* (5), 2483-2491.
11. Bentley, C. L.; Kang, M.; Unwin, P. R., Scanning Electrochemical Cell Microscopy: New Perspectives on Electrode Processes in Action. *Current Opinion in Electrochemistry* **2017,** *6* (1), 23-30.
12. Bentley, C. L.; Edmondson, J.; Meloni, G. N.; Perry, D.; Shkirskiy, V.; Unwin, P. R., Nanoscale Electrochemical Mapping. *Analytical Chemistry* **2019,** *91* (1), 84-108.
13. Ebejer, N.; Güell, A. G.; Lai, S. C. S.; McKelvey, K.; Snowden, M. E.; Unwin, P. R., Scanning Electrochemical Cell Microscopy: A Versatile Technique for Nanoscale Electrochemistry and Functional Imaging. *Annu. Rev. Anal. Chem.* **2013,** *6*, 329-351.
14. Chen, C.-H.; Jacobse, L.; McKelvey, K.; Lai, S. C. S.; Koper, M. T. M.; Unwin, P. R., Voltammetric Scanning Electrochemical Cell Microscopy: Dynamic Imaging of Hydrazine Electro-oxidation on Platinum Electrodes. *Analytical Chemistry* **2015,** *87* (11), 5782-5789.
15. Bentley, C. L.; Unwin, P. R., Nanoscale Electrochemical Movies and Synchronous Topographical Mapping of Electrocatalytic Materials. *Faraday Discussions* **2018,** *210*, 365-379.
16. Bentley, C. L.; Kang, M.; Unwin, P. R., Nanoscale Structure Dynamics within Electrocatalytic Materials. *J. Am. Chem. Soc.* **2017,** *139* (46), 16813-16821.
17. Byers, J. C.; Nadappuram, B. P.; Perry, D.; McKelvey, K.; Colburn, A. W.; Unwin, P. R., Single Molecule Electrochemical Detection in Aqueous Solutions and Ionic Liquids. *Analytical Chemistry* **2015,** *87* (20), 10450-10456.
18. Bard, A. J.; Faulkner, L. R.; White, H. S., Electrochemical methods : fundamentals and applications. Third edition. ed.; Wiley,: Hoboken, NJ, 2022; p. 1 online resource.